Archives of Razi Institute Journal
"Arch. Razi Inst."

Journal Homepage: https://archrazi.areeo.ac.ir/

Original Article

Enhanced Vaccine Design Strategies for Toxoplasmosis: A Computational Analysis of *Toxoplasma gondii* Rhoptry Protein 13 (ROP13)

Leila Zaki[1], Aida Vafae Eslahi[1], Masoud Foroutan[2,3], Majid Pirestani[4], Kareem Hatam-Nahavandi[5], Amir Karimipour-saryazdi[4], Mohammad Ghaffari Cherati[1], Daniel Diaz[6], Milad Badri[1*]

1. Medical Microbiology Research Center, Qazvin University of Medical Sciences, Qazvin, Iran.
2. Research Center for Environmental Contaminants (RCEC), Abadan University of Medical Sciences, Abadan, Iran.
3. Department of Basic Medical Sciences, Faculty of Medicine, Abadan University of Medical Sciences, Abadan, Iran.
4. Department of Parasitology and Entomology, Faculty of Medical Sciences, Tarbiat Modares University, Tehran, Iran.
5. Department of Parasitology and Mycology, School of Medicine, Iranshahr University of Medical Sciences, Iranshahr, Iran.
6. Faculty of Sciences, National Autonomous University of Mexico, Mexico City, Mexico.

Use your device to scan and read the article online

How to cite this article Zaki L, Vafae Eslahi A, Foroutan M, Pirestani M, Hatam-Nahavandi K, Karimipour-saryazdi A, et al. Enhanced Vaccine Design Strategies for Toxoplasmosis: A Computational Analysis of *Toxoplasma gondii* Rhoptry Protein 13 (ROP13). Archives of Razi Institute Journal. 2025; 80(5):1301-1320. https://doi.org/10.32598/ARI.80.5.3301

https://doi.org/10.32598/ARI.80.5.3301

Article info:
Received: 23 Mar 2025
Accepted: 14 Jun 2025
Published: 01 Sep 2025

Keywords:
In silico, Rhoptry protein 13, *Toxoplasma gondii*

ABSTRACT

Introduction: *Toxoplasma gondii*, an intracellular parasite, utilizes a variety of rhoptry proteins (ROPs) to facilitate invasion and interaction with host cells. Among these ROPs, rhoptry protein 13 (ROP13) stands out for its expression in both bradyzoite and tachyzoite forms of *T. gondii* and its ability to engage with various host cytoplasmic compartments.

Materials & Methods: In this bioinformatics study, we employed a range of tools to predict the fundamental characteristics of the ROP13 protein.

Results: Our analysis revealed that the ROP13 protein consists of 400 amino acid residues with an average molecular weight (MW) of 44,714.15 daltons. The grand average of hydropathicity (GRAVY) was determined to be -0.311, indicating the protein's hydrophilic nature, while the aliphatic index scored 84.40, highlighting its hydrophobic character. Furthermore, we identified 43 post-translationally modified sites within the ROP13 sequence. When examining the secondary structure, the ROP13 protein was predicted to have a composition of 40% alpha helix, 9.25% extended strand, and 50.75% random coil using the GOR4 method, suggesting a diverse structural organization that may contribute to its functional versatility. Additionally, our analysis identified several potential B- and T-cell epitopes within the ROP13 sequence, indicating regions that could be targeted for immune responses.

*** Corresponding Author:**
Milad Badri, Assistant Professor.
Address: *Medical Microbiology Research Center, Qazvin University of Medical Sciences, Qazvin, Iran.*
Tel: *+98 (911) 4649388*
E-mail: *badri22.milad@gmail.com*

Archives of Razi Institute Journal

Conclusion: The bioinformatics analysis of ROP13 provides valuable insights into its structural, immunogenic, and antigenic properties, highlighting its potential as a target for vaccine development against toxoplasmosis. By leveraging the predicted characteristics of ROP13, researchers can explore various vaccine strategies to enhance host immunity and combat *T. gondii* infection effectively. Continued investigation into the molecular mechanisms underlying ROP13's interactions with host cells will further elucidate its role in *T. gondii* pathogenesis and guide the development of innovative approaches to mitigate this prevalent parasitic disease.

1. Introduction

Toxoplasma gondii is a widely distributed protozoan parasite posing a significant public health concern, with an estimated one-third of the global population exposed to this parasite [1, 2].

The life stages of *T. gondii* consist of a sexual phase and an asexual phase, which occur exclusively in feline species (definitive hosts) and any warm-blooded animal (intermediate hosts), respectively [3-5]. Oocysts, shed through the feces of definitive hosts, serve as the infectious stage of *T. gondii*. Environmental contamination of soil and water are the primary sources of infection [6]. Accordingly, humans acquire the infection via contaminated drinking water or food, consumption of raw or undercooked meats containing latent cysts, vertical transmission, organ transplantation, and blood transfusion [6, 7].

The clinical characteristics of toxoplasmosis are influenced by various factors, including the genotype of the protozoan and host-related characteristics such as age, sex, occupation, genetics, diet, immunological status, cultural behaviors, and contact with infected cats [8-10].

In immunocompetent individuals, *T. gondii* generally causes mild clinical manifestations, such as flu-like symptoms, while in some individuals with compromised immune status (patients with HIV/AIDS, seronegative pregnant women, and organ transplant recipients), *T. gondii* infections can cause serious disease, such as encephalitis, intellectual disability, vision disorders, hydrocephalus, cerebral calcification, poor coordination, or may lead to death if not treated [11, 12]. *T. gondii* infection can lead to frequent abortions, stillbirths, the birth of debilitated animals, and fetal death in some domestic animals, particularly sheep and goats. These outcomes result in significant economic disadvantages in animal husbandry settings and veterinary-related industries [13].

Toxoplasmosis is typically treated with chemotherapy that includes antimalarial and antibacterial medications, which are the recommended drugs for managing the disease. Nevertheless, these agents have not been completely successful and can have harmful side effects such as teratogenic effects, hypersensitivity, tissue damage, significant toxicity, potential parasite resistance, as well as bone marrow suppression [14, 15].

Since antiparasitic drugs have some limitations and are unable to eradicate bradyzoites in tissue cysts, the discovery and design of safe and effective vaccines are needed, particularly for humans and livestock animals. One of the significant challenges facing scientists in addressing *T. gondii* infection is the development of a useful and effective vaccine. To address this challenge, various immunization approaches with different formulations have been explored for toxoplasmosis. Recent vaccine development trials aimed at preventing *T. gondii* infection have primarily focused on antigens found on the parasite's major surface (SAGs), as well as proteins from micronemes (MICs), rhoptries (ROPs), and dense granules (GRAs) [16-19].

Among these different antigens, the ROP protein family is a romising vaccine candidate due to its strong antigenicity and immunogenicity, as well as its ability to induce substantial immune responses [20, 21]. Several studies have assessed the efficacy of ROP antigens using different vaccine platforms, such as recombinant protein or DNA vaccines, in animal models to obtain favorable and promising results [18-21]. As an excretory-secretory protein of *T. gondii*, ROP13 has the ability to modulate immune response and therefore shows great promise for application in immunization approaches against the infection [21]. Furthermore, this protein exhibits strong immunogenicity similar to other ROPs and plays a crucial role in pathogenicity and survival within host cells [21-24].

Using in silico tools to predict vaccine targets is highly valuable, as it enhances our understanding of these targets and allows for their rapid selection with careful consideration [25, 26]. Bioinformatics is the most successful prediction method for identifying effective epitopes and developing vaccines [25]. These novel techniques are highly beneficial for analyzing proteins and assessing their structural, functional, immunogenic, biological, and biochemical characteristics as antigens [19, 26]. Therefore, the present study was designed to identify the essential biochemical characteristics and immunogenic epitopes of the ROP13 protein by utilizing various bioinformatics online servers.

2. Materials and Methods

2.1. Retrieval and initial assessment of the protein sequence

Initially, the amino acid sequence of ROP13 was obtained from the National Center for Biotechnology Information (NCBI) website in FASTA format [27].

2.2. Analysis of the physicochemical parameters of ROP13

The Expasy ProtParam tool [28] was utilized to assess various physicochemical characteristics of ROP13, including amino acid composition, theoretical isoelectric point (pI), molecular weight (MW), total number of positively and negatively charged residues, extinction coefficients, instability index, aliphatic index, grand average of hydropathicity (GRAVY), and in vitro and in vivo half-life [29].

2.3. Projecting the post-translational modification (PTM) sites on ROP13

The online tools NetPhos 3.1 [30] and CSS-Palm [31] were used to determine the phosphorylation and acylation regions of the ROP13 protein, respectively [25].

2.4. The transmembrane domains and subcellular position of ROP13

The potential transmembrane regions (TMs) of ROP13 were evaluated using TMHMM 2.0 [32]. Additionally, the subcellular position of the protein was predicted using PSORT II [33, 25].

2.5. The secondary and tertiary structure prediction

The secondary structure of ROP13 was predicted using the Garnier-Osguthorpe-Robson (GOR) method through the online server [34, 35]. Afterward, the three-dimensional (3D) models of the ROP13 sequence were generated using the SWISS-MODEL program, based on a homology modeling approach [25, 36, 37].

2.6. Refinement and confirmation of the 3D modeled structure

The precision and quality of the generated models were determined using a Ramachandran plot through the PROCHECK tool, available on the SAVES v6.0 server [38-40].

2.7. B-cell epitopes prediction

To predict B-cell epitopes, the amino acid sequence of the ROP13 protein (accession no. AFH54221.1) was utilized. The ABCpred online server [41] was employed with a threshold of 0.5 to identify linear B-cell epitopes within the antigen sequence [42]. To predict B-cell epitopes, we utilized the Bcepred tool, which identifies continuous B-cell epitopes based on physicochemical properties such as accessibility, polarity, hydrophilicity, turns, exposed surface, flexibility, and antigenic propensity [43, 44].

Besides, the IEDB tool from the Immune Epitope Database [45] was employed to evaluate epitopes based on average flexibility, hydrophobicity, surface accessibility, antigenicity, alpha-helix, and beta-turn. Eventually, conformational B-cell epitopes were evaluated using ElliPro [46] based on the 3D epitope structure from the protein data bank file using default parameters: a minimum score of 0.5 and a maximum distance of 6 Å. This server predicts the epitopes based on their protusion index (PI) values to estimate protein shape, residue-level PI, and adjacent cluster residues [47].

2.8. MHC-I and MHC-II binding epitopes prediction

The Immune Epitope Database (IEDB) [48] was used to assess the half maximal inhibitory concentration (IC_{50}) of peptides derived from ROP13 that exhibit affinity to both major histocompatibility complex (MHC) class I and class II molecules. The procedure utilized the IEDB-recommended prediction methods, accessible through the links for both MHC class I and MHC class II [49, 50].

The MHC-I epitopes, each consisting of ten amino acids, were predicted using the mouse alleles H2-Ld, H2-Db, H2-Dd, H2-Kb, H2-Kd, and H2-Kk. For MHC-II epitope prediction, which involved 15 amino acids, the

mouse alleles H2-IAb, H2-IAd, and H2-IEd were employed. The predictions were ranked according to percentile scores [51, 52].

2.9. Cytotoxic T lymphocyte (CTL) epitopes prediction

Identification of cytotoxic T-cell epitopes was accomplished using the CTLpred tool, which has a reported prediction accuracy of 75.8% [53]. The prediction was performed using a previously described consensus approach. Default parameters included a support vector machine (SVM) score of 0.36 and an artificial neural network (ANN) score of 0.51 [54].

2.10. Evaluation of antigen probability, allergenicity, and solubility

The full antigenicity of the ROP13 protein was initially assessed using ANTI¬GENpro [55, 56], and subsequently evaluated with VaxiJen v. 2.0 [57, 58], both of which are web-base servers.

VaxiJen is used to predict conserved antigenic regions and employs a novel alignment-free approach based on auto-cross covariance (ACC), which evaluates variations in peptide sequences to generate comparable vectors of primary amino acid features. Its prediction accuracy ranges between 70% and 89%, depended on the target organism [57].

Furthermore, the allergenic profile of ROP13 was predicted using the AlgPred [59, 60], employing a hybrid methodology that combines SVMc, IgE epitope prediction, ARPs BLAST, and MAST. AlgPred predicts epitopes with up to 85% accuracy by comparing identified epitopes with protein regions, using a threshold of -0.4. The solubility of ROP13 was assessed using the SOLpro server [61].

2.11. Immune simulation

C-ImmSim was employed to simulate the virtual immunological response triggered by TgROP13 [62]. The simulation was configured for three inoculation doses of TgROP13 administered at four-week interval, corresponding to time points 1, 84, and 168. Additional parameters included a simulation volume of 10, 1050 simulation steps, and random seed of 12345 [63, 64].

3. Results

3.1. Gene and overall features of ROP13

The amino acid sequence of the ROP13 protein was acquired from NCBI in FASTA format (accession No. AFH54221.1).

According to ProtParam, the ROP13 protein consists of 400 amino acid residues with a predicted pI of 9.38 and a molecular weight of 44,714.15 Da. The ROP13 sequence contains 45 negatively charged residues (Asp + Glu) and 56 positively charged residues (Arg + Lys).

The extinction coefficient was measured to be 20440 M−1 cm−1 in water at 280 nm.

The estimated half-life of ROP13 was 30 hours in mammalian reticulocytes in vitro, over 20 hours in yeast in vivo, and over 10 hours in *Escherichia coli* in vivo.

Table 1. The acylation sites of ROP13 sequence

ID	Position	Peptide	HAT	Score	Cutoff
AFH54221.1	2	******MKRTELCIA	EP300	1.3	0.42
AFH54221.1	2	******MKRTELCIA	KAT2B	1.807	1.343
AFH54221.1	2	******MKRTELCIA	KAT8	8.9	7.222
AFH54221.1	82	TSRPPGRKYEGSDLH	KAT2A	1.638	1.382
AFH54221.1	82	TSRPPGRKYEGSDLH	KAT2B	1.798	1.343
AFH54221.1	100	AARHVEHKKRQEEWE	KAT8	7.5	7.222
AFH54221.1	101	ARHVEHKKRQEEWEQ	KAT2B	1.413	1.343
AFH54221.1	101	ARHVEHKKRQEEWEQ	KAT5	1.094	0.71
AFH54221.1	253	KSEEFTRKVNRCSED	KAT2A	1.493	1.382

```
      MKRTELCIAALVAVGAFAFTSPNAVAKSFERSLGHLDASSFLSSPLNSDV   #     50
      ELGRSTSPAQSPSFTEGTNETNPPTSRPPGRKYEGSDLHRRVAARHVEHK   #     100
      KRQEEWEQRKASRRSALTPSAPDPDGDGDPATSFPSQRRLLDRCLQQFRE   #     150
      QLVDWENLCKGSPEPDDCRSTVQEILANQSFGALHTTVISFSIFVNRDPR   #     200
      RLSFPVLDATDLRLTVKLKHLLDRIPGCAALSLPAYIGLVSSDVFKSEEF   #     250
      TRKVNRCSEDFGRSAREEPSRAGRAAAVVIRFMGLTPERQTFYQPFVFVT   #     300
      TQAAMLLSMVLKHPFLSILVNMACVAGGLCRKGIREVLLRALREADFQTE   #     350
      DVPLDSAPQELVDHLKMYLKLLFLRKYRRLRRQAANVAAQVVYANSLRLL   #     400
%1    ...T..............T.......S...S......SS..SS...S..   #      50
%1    .....TS...S.S.T.........TS.........................   #     100
%1    ...........S..S..T.S...........TS..S...............   #     150
%1    ...........S........T........S.....................   #     200
%1    ..S...........T................S........SS....S...   #     250
%1    T......S.....S.....................T....T.........   #     300
%1    T...............S................................T.   #     350
%1    ...............................................S....   #     400
```

A.

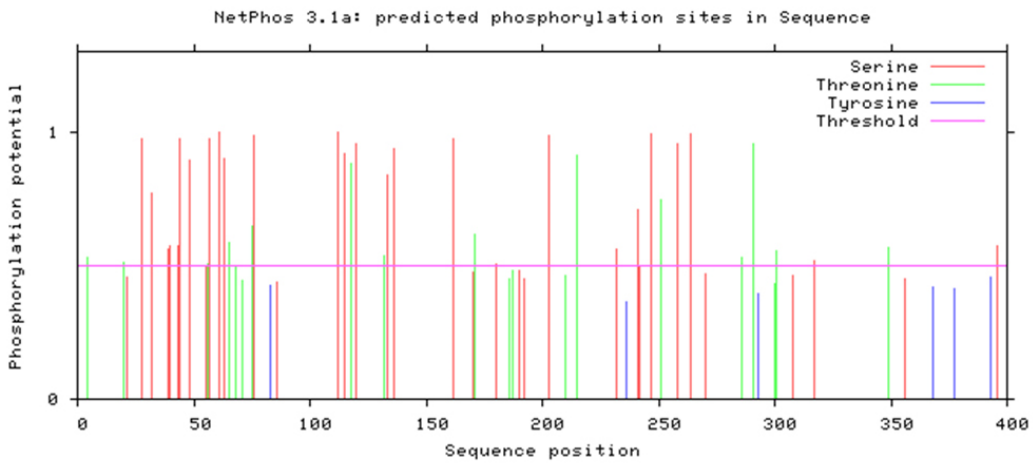

B.

Figure 1. Bioinformatics analysis of the phosphorylation and acylation areas of the ROP13

A) If the residue is not phosphorylated, either because the score is below the threshold or because the residue is not S (serine), T (threonine), or Y (tyrosine), that position is marked by a dot ('.'); Residues having a prediction score above the threshold are indicated by 'S', 'T', or 'Y', respectively; B) Expected phosphorylation positions in the ROP13 sequence

Moreover, the instability index (II) of this protein indicates its unstable nature, with a score of 61.30. In addition, the GRAVY and aliphatic index were calculated to be -0.311 and 84.40, respectively.

3.2. PTM sites prediction on ROP13

The results revealed that the ROP13 protein contains 41 phosphorylation sites (27 Ser, 14 Thr, and 0 Tyr) as shown in Figures 1A and 1B, along with two acylation sites listed in Table 1, indicating that there are a total of 43 PTM sites within our sequence.

3.3. Forecasting TMs and subcellular localization of ROP13

According to TMHMM results, one transmembrane domain was observed in the ROP13 sequence (Figure 2). In addition, using the PSORT II program [33], the ROP13 subcellular localization was determined as follows: 33.3% plasma membrane, 22.2% endoplasmic reticulum, 33.3% Golgi, and 11.1% extracellular, including the cell wall.

3.4. Assessment of secondary and tertiary structure

```
# AFH54221.1 Number of predicted TMHs:  1
# AFH54221.1 Exp number of AAs in TMHs: 20.38952
# AFH54221.1 Exp number, first 60 AAs:  16.79055
# AFH54221.1 Total prob of N-in:        0.84813
# AFH54221.1 POSSIBLE N-term signal sequence
# AFH54221.1      TMHMM2.0  inside        1   6
# AFH54221.1      TMHMM2.0  TMhelix       7   26
# AFH54221.1      TMHMM2.0  outside       27  400
```

A.

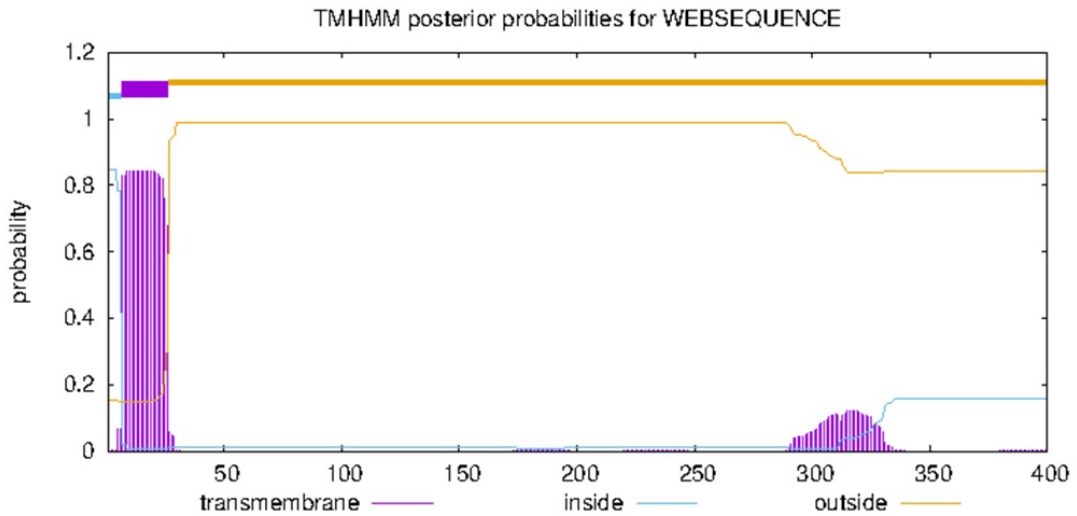

B.

Figure 2. Bioinformatic analysis of the transmembrane domain of the ROP13 sequence [32].

A) Number of predicted TMHs: The number of predicted transmembrane helices

Note: Exp number of AAs in TMHs: The expected number of amino acids in transmembrane helices. If this number is larger than 18, it is very likely to be a transmembrane protein (OR have a signal peptide); Exp number, first 60 AAs: The expected number of amino acids in transmembrane helices in the first 60 amino acids of the protein. If this number is more than a few, you should be warned that a predicted transmembrane helix in the N-term could be a signal peptide; Total probability of N-in: The total probability that the N-term is on the cytoplasmic side of the membrane; POSSIBLE N-term signal sequence: a warning that is produced when "Exp number, first 60 AAs" is larger than 10 [68].

B) Graphical illustration of transmembrane domain analysis of ROP13

The GOR4 analysis showed that the secondary structure of the ROP13 protein consists of 400 amino acids and comprises 40% alpha helix (H) (160/400), 50.75% random coil (203/400), and 9.25% extended strand (37/400) (Figure 3). The SWISS-MODEL findings are fully depicted in Figure 4.

3.5. Verification of the 3D model structure

The quality of the modeled structure was validated by representing the percentage of residues in disallowed and allowed areas (Figure 5).

```
        10        20        30        40        50        60        70
        |         |         |         |         |         |         |
MKRTELCIAALVAVGAFAFTSPNAVAKSFERSLGHLDASSFLSSPLNSDVELGRSTSPAQSPSFTEGTNE
ccccchhhhhhhhccccccccchhhhhhhhhccccccccccccccccccccccccccccccccccccc
TNPPTSRPPGRKYEGSDLHRRVAARHVEHKKRQEEWEQRKASRRSALTPSAPDPDGDGDPATSFPSQRRL
ccccccccccccccccchhhhhhhhhhhhhhhhhhhhhhhhhhhcccccccccccccccccccccchhhhh
LDRCLQQFREQLVDWENLCKGSPEPDDCRSTVQEILANQSFGALHTTVISFSIFVNRDPRRLSFPVLDAT
hhhhhhhhhhceecceeecccccccccccchhhhhhhhhcccccccceeeeeeecccccccccccccchh
DLRLTVKLKHLLDRIPGCAALSLPAYIGLVSSDVFKSEEFTRKVNRCSEDFGRSAREEPSRAGRAAAVVI
hhhhhhhhhhhhccccccccccccceeeeecccccchhhhheeecccccccccccccchhhhhhhhhhh
RFMGLTPERQTFYQPFVFVTTQAAMLLSMVLKHPFLSILVNMACVAGGLCRKGIREVLLRALREADFQTE
hhccccccccccccceeeehhhhhhhhhhhcccceeeeeeeeecccccccchhhhhhhhhhhhccccc
DVPLDSAPQELVDHLKMYLKLLFLRKYRRLRRQAANVAAQVVYANSLRLL
ccccccchhhhhhhhhhhhhhhhhhhhhhhhhhhhhhhhhhhhccceeec
```

A.

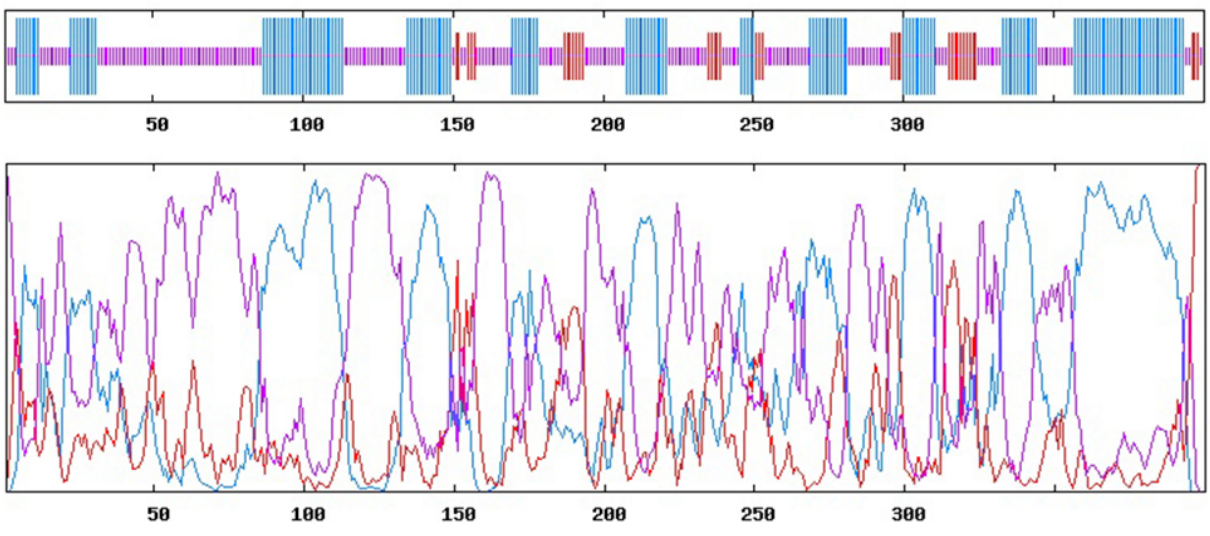

B.

Figure 3. A) Predicted secondary structure by the GOR IV online service [70]; B) Graphical results for secondary structure prediction of ROP13 protein by GOR IV

Note: h: Helix, e: Extended strand, c: Coil.

The analysis of Ramachandran plot statistics revealed that 91.8% of amino acid residues from the structure modeled by SWISS-MODEL were incorporated in the favored regions; while only 7.6% and 0.6% were in the allowed and disallowed regions of the plot, respectively.

3.6. B-cell epitopes prediction

Table 2 displays the results obtained from the Bcepred web server. Additionally, Table 3 presents the high-score 16-mer linear B-cell epitopes identified using ABCpred. Only epitopes with a score higher than 0.5 are included in Table 3.

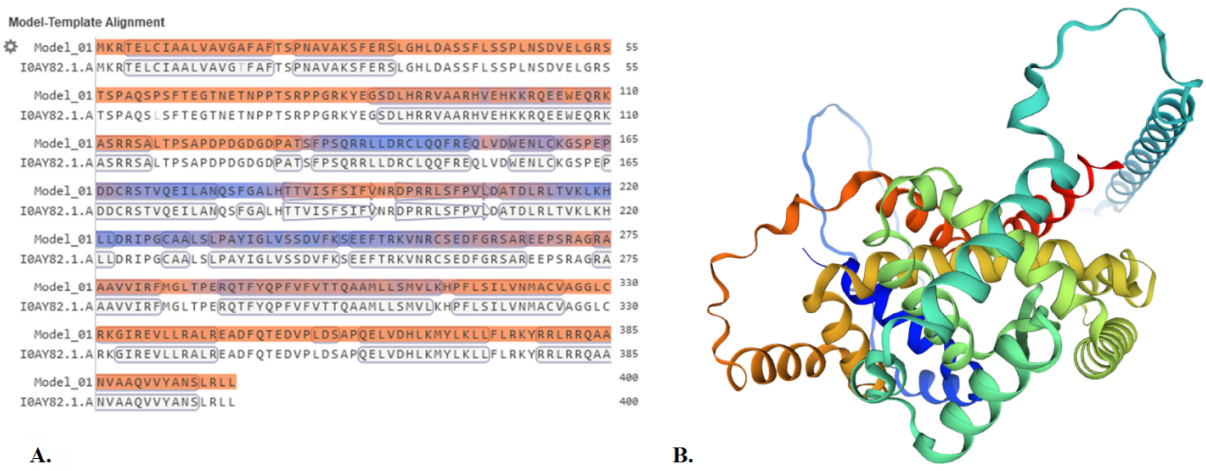

Figure 4. Output of SWISS-MODEL, online server [36]

A) Sequence identity and Model alignment; B) The 3D model constructed for the ROP13 protein

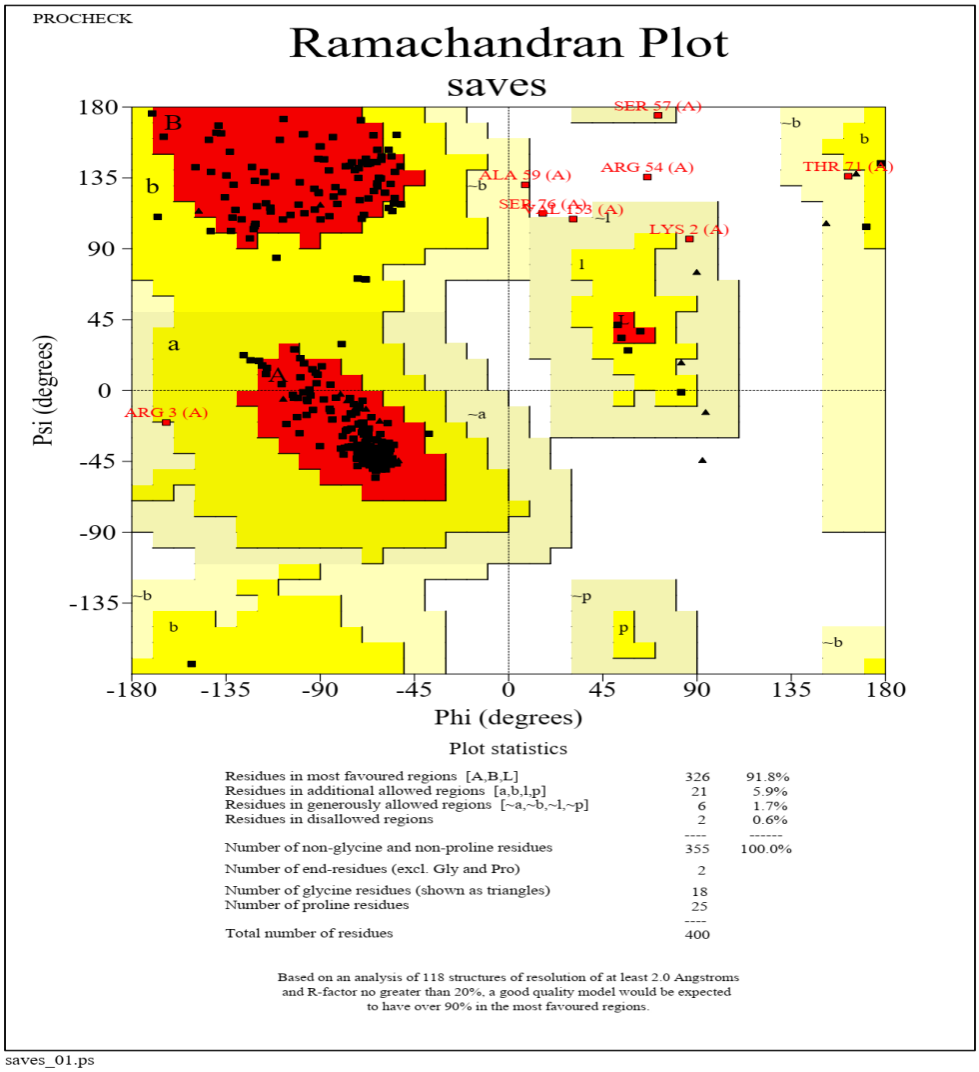

Figure 5. ROP13 protein 3D structure confirmation using the Ramachandran plot, [38]

Table 2. Epitopes predicted in the ROP13 protein using different parameters based on the Bcepred online server

Prediction Parameter	Epitope Sequence
Flexibility	AVAKSFE; SFLSSPL; DVELGRSTS; PSFTEGTNETNPPTSRPPGRKYE; RHVEHKKRQEEWEQRKASRR; ENLCKGSPEPDDCR; IFVNRDP; EEFTRKVNRCSEDFGRSAREEPSRA; GLCRKGI; RKYRRLR
Hydrophilicity	GRSTSPAQSPS; TEGTNETNPPTSR; GRKYEGSD; EHKKRQEE; EQRKASRRSA; PSAPDPDGDGDPATS; CKGSPEPDDCRSTV; VNRCSEDFGRSAREEPSRAGR; ADFQTED
Accessibility	AKSFERSL; TSFPSQRRLLDR; LQQFREQL; KGSPEPDDCRST; FVNRDPRRLSFP; RSTSPAQSPSFTEGTNETNPPTSRPPGRKYEGSDLHRRVAARHVEHKKRQEEWEQRKASRRSALTPSAPDPDGDGDP; DVFKSEEFTRKVNRCSE; FGRSAREEPSRAGR; GLTPERQTFYQP; CRKGIREV; RALREADFQTED; LFLRKYRRLRRQAANV;
Turns	-
Exposed surface	-
Polarity	MKRTELCI; VAKSFERSLGHL; QRRLLDRC; PEPDDCRS; LCRKGIREVLLRALREAD; SRPPGRKYEGSDLHRRVAARHVEHKKRQEEWEQRKASRRSA; DPDGDGD; QRRLLDRC; VNRDPRRLS; RLTVKLKHLLDRI; DVFKSEEFTRKVNRCSE; FGRSAREEPSRAGR; ELVDHLKMYLKLLFLRKYRRLRRQAA;
Antigenic propensity	SFLSSPL; RLLDRCLQQ; LHTTVISFSIFV; RLSFPVLD; LRLTVKLKHLL; YIGLVSSDVFK; TFYQPFVFVTTQ; MLLSMVLKHPFLSILVNM; GIREVLLR; QELVDHLKMYLKLLFLRKY

The graphical prediction of continuous B-cell epitopes for ROP13 was conducted using the following threshold values for different parameters: Bepipred linear (0.502), hydrophilicity (1.471), flexibility (1.000), antigenicity (1.038), beta-turn (0.966), and surface accessibility (1.000) (Figure 6). Fourteen discontinuous B-cell epitopes were predicted using the ElliPro server (Table 4).

3.7. MHC-I and MHC-II binding epitope prediction

The T-cell epitopes with the lowest IC_{50} values (or percentile ranks) were selected. The minimum percentile scores for each MHC allele for ROP13 are presented in Tables 5 and 6.

3.8. CTL epitope prediction

The ten highest ranked CTL epitopes of the ROP13 protein were identified and are presented in Table 7.

3.9. Antigenicity, allergenicity, immune simulation profile, and solubility assessment

The antigenicity scores of ROP13 were calculated as 0.821125 and 0.5796 using ANTIGENpro and VaxiJen v.2.0, respectively. A threshold value of 0.5 was considered for both models. According to simulations from the C-ImmSim server, TgROP13 has the potential to trigger both humoral and cell-mediated immune responses, as indicated by the predicted antibody levels and cytokine patterns following antigen administration (data not shown).

The findings from the AlgPred server, using the hybrid approach, demonstrated that the ROP13 protein is non-allergenic.

The solubility of the ROP13 protein after overexpression in *E. coli* was predicted to be 0.7847.

4. Discussion

Toxoplasmosis is now widely recognized as one of the main threats to human society and the livestock industry that lacks a global solution [6, 7, 13]. So far, no vaccine or appropriate treatment is available to prevent and control this infectious disease. Furthermore, the existing drugs are not entirely satisfactory and can induce adverse side effects in patients [7, 14]. Hence, the quest to develop an effective and safe vaccine specifically targeting toxoplasmosis has been a key area of research for scientists around the world [65].

Designing successful vaccines with conventional methods is expensive, tedious, and takes considerable time. In silico is the most successful technology for the identification of accurate biomarkers to guide treatment selection that can significantly reduce both time and cost of diagnosis [66]. Research has demonstrated that the ROP family has a critical impact on the invasion of *T. gondii* and its interaction with host cells [20, 21]. The ROP13 protein has the ability to enter the cytoplasm of host cells, demonstrating strong immunogenicity and pathogenicity [22].

Table 3. Linear B-cell epitopes predicted from the full-length ROP13 protein using the ABCpred server

Rank	Sequence	Start Position	Score
1	VQEILANQSFGALHTT	172	0.91
2	SSDVFKSEEFTRKVNR	241	0.90
3	RRVAARHVEHKKRQEE	90	0.88
4	ENLCKGSPEPDDCRST	156	0.87
5	PSAPDPDGDGDPATSF	119	0.86
6	RRSALTPSAPDPDGDG	113	0.85
7	TNPPTSRPPGRKYEGS	71	0.83
7	TPERQTFYQPFVFVTT	286	0.83
7	AGRAAAVVIRFMGLTP	272	0.83
8	PAQSPSFTEGTNETNP	58	0.81
8	AVGAFAFTSPNAVAKS	13	0.81
8	DGDGDPATSFPSQRRL	125	0.81
8	EEWEQRKASRRSALTP	104	0.81
9	SFSIFVNRDPRRLSFP	190	0.79
10	RPPGRKYEGSDLHRRV	77	0.78
11	LFLRKYRRLRRQAANV	372	0.75
11	LPAYIGLVSSDVFKSE	233	0.75
12	PQELVDHLKMYLKLLF	358	0.74
12	PGCAALSLPAYIGLVS	226	0.74
12	SFPSQRRLLDRCLQQF	133	0.74
13	YEGSDLHRRVAARHVE	83	0.73
13	ALREADFQTEDVPLDS	341	0.73
14	RSAREEPSRAGRAAAV	263	0.71
14	QFREQLVDWENLCKGS	147	0.71
15	TVKLKHLLDRIPGCAA	215	0.70
16	GGLCRKGIREVLLRAL	327	0.69
17	LGHLDASSFLSSPLNS	33	0.68
18	SSFLSSPLNSDVELGR	39	0.67
18	LSMVLKHPFLSILVNM	307	0.67
19	ELCIAALVAVGAFAFT	5	0.66
19	SDVELGRSTSPAQSPS	48	0.66
19	SILVNMACVAGGLCRK	317	0.66

Rank	Sequence	Start Position	Score
20	NRDPRRLSFPVLDATD	196	0.65
21	VTTQAAMLLSMVLKHP	299	0.61
22	RLRRQAANVAAQVVYA	379	0.60
23	FPVLDATDLRLTVKLK	204	0.59
24	YQPFVFVTTQAAMLLS	293	0.58
25	NAVAKSFERSLGHLDA	23	0.52

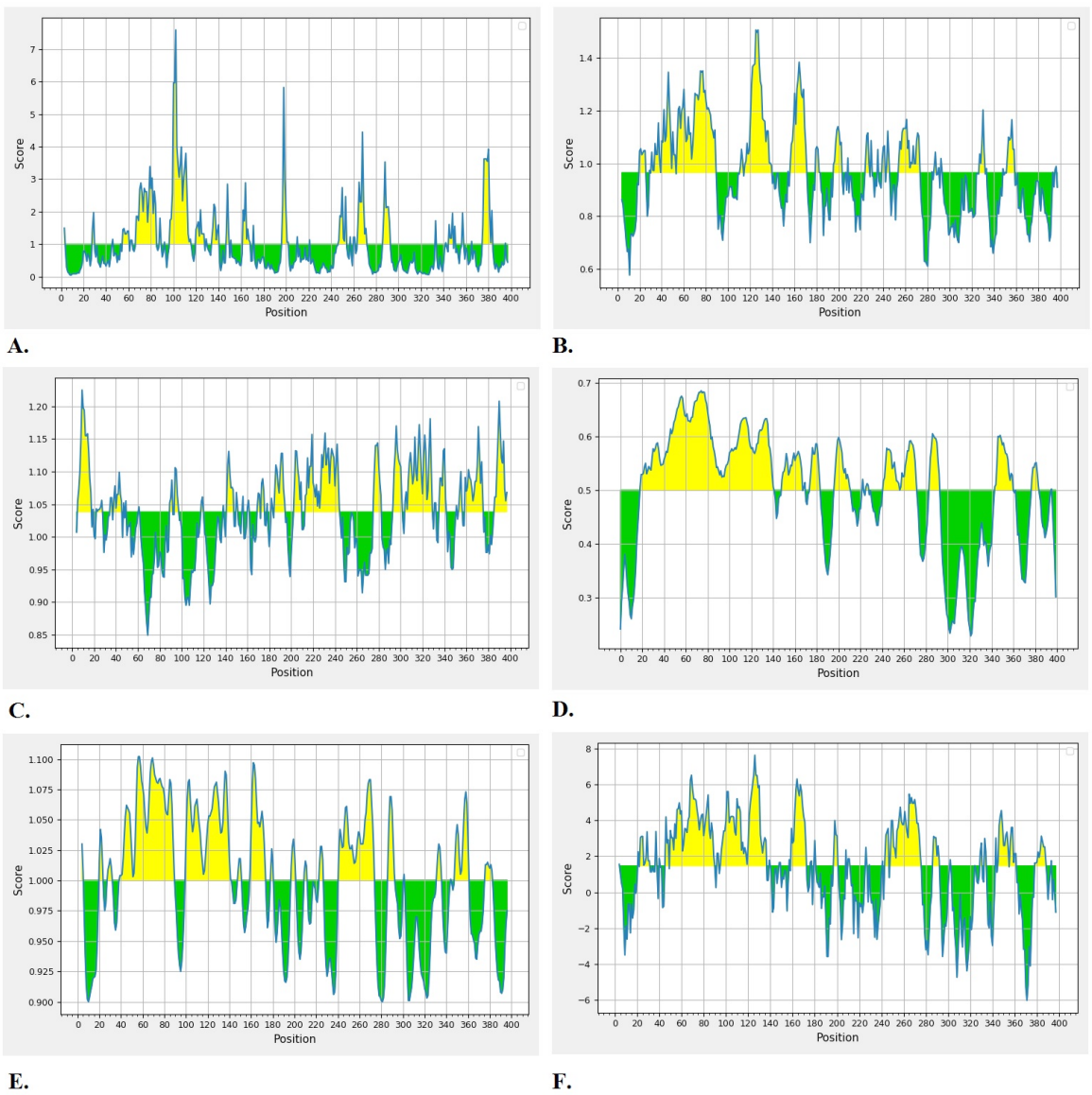

Figure 6. Linear B-cell epitopes of the ROP13 protein sequence predicted by the ProtScale server [28], based on percent accessibility (A), beta-turn (B), antigenicity (C), bepipred linear (D), flexibility (E), and hydrophilicity (F)

Note: The horizontal line indicates the threshold or the average score. Yellow regions (above the threshold) indicate favorable areas related to the properties of interest. Green regions (below the threshold) indicate unfavorable areas related to the properties of interest.

Table 4. Conformational B cell epitopes of the TgROP13 protein predicted using the ElliPro server

No.	Residues	Number of Residues	Score	3D Structure
1	A:R77, A:P78, A:P79, A:G80, A:R81 (RPPGR)	5	0.958	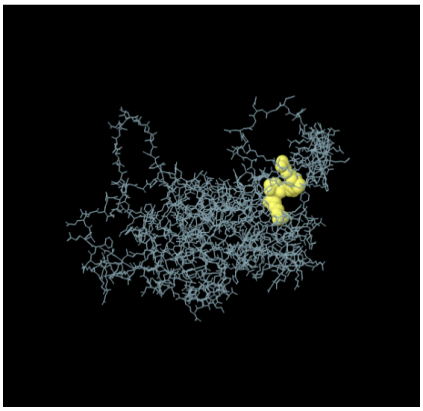
2	A:L42, A:S43, A:S44, A:P45, A:L46, A:N47, A:S48, A:D49, A:V50, A:E51, A:L52, A:G53, A:R54, A:S55, A:T56, A:S57, A:P58, A:A59, A:Q60, A:S61, A:P62, A:S63, A:F64, A:T65, A:E66, A:G67, A:T68, A:N69, A:E70, A:T71, A:N72, A:P73, A:P74, A:T75, A:S76 (LSSPLNSDVELGRSTSPAQSPS-FTEGTNETNPPTS)	35	0.921	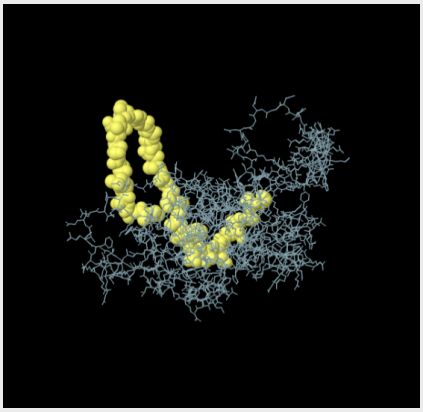
3	A:E84, A:G85, A:S86, A:D87, A:L88, A:H89, A:R90, A:R91 (EGSDLHRR)	8	0.893	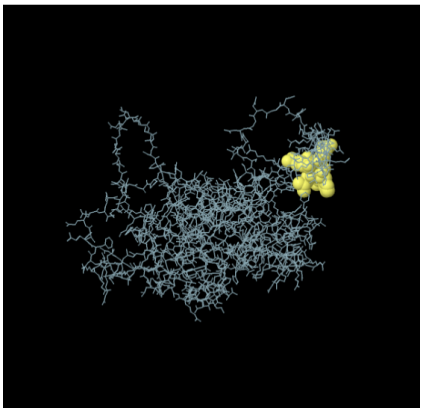
4	A:V92, A:A93, A:A94, A:R95, A:H96, A:V97, A:E98, A:H99, A:K100, A:K101, A:R102, A:Q103, A:E104, A:E105, A:W106, A:R109 (VAARHVEHKKRQEEWR)	16	0.779	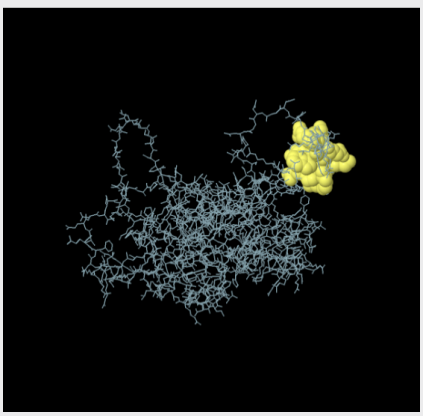

No.	Residues	Number of Residues	Score	3D Structure
5	A:E107, A:K110, A:A111, A:S112, A:R113, A:R114, A:S115, A:A116, A:L117, A:T118, A:P119, A:S120, A:A121, A:P122, A:D123, A:P124, A:D125, A:G126, A:D127, A:G128, A:D129, A:P130, A:A131, A:T132, A:S133, A:P135, A:S136, A:R139 (EKASRRSALTPSAPDPDGDG-DPATSPSR)	28	0.773	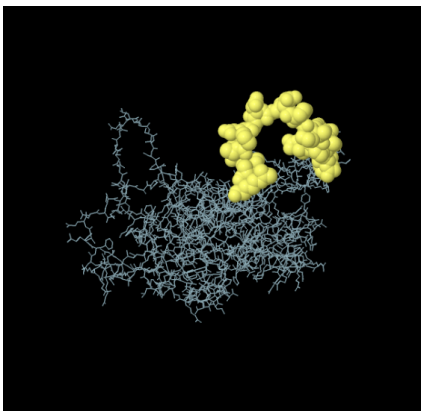
6	A:L36, A:D37, A:A38, A:S39, A:S40, A:F41 (LDASSF)	6	0.742	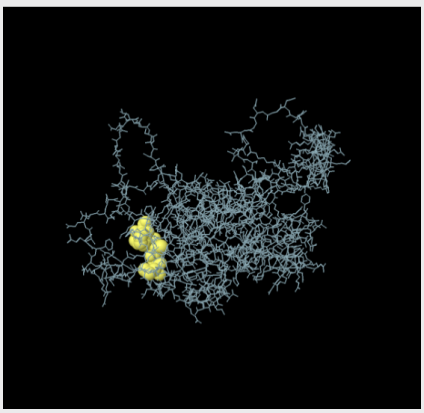
7	A:Q348, A:T349, A:E350, A:D351, A:V352, A:P353, A:L354, A:D355, A:S356, A:A357 (QTEDVPLDSA)	10	0.708	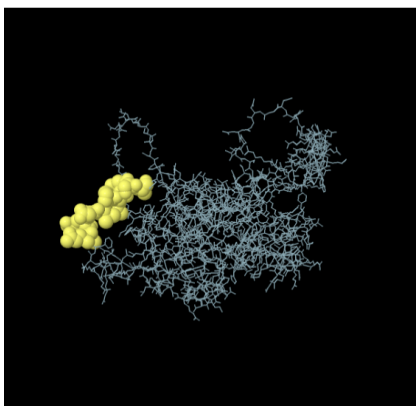
8	A:A326, A:G327, A:G328, A:L329, A:C330, A:G333, A:I334, A:R335, A:E336, A:V337, A:L338, A:L339, A:R340, A:A341, A:L342, A:R343, A:E344, A:A345, A:D346, A:F347 (AGGLCGIREVLLRALREADF)	20	0.679	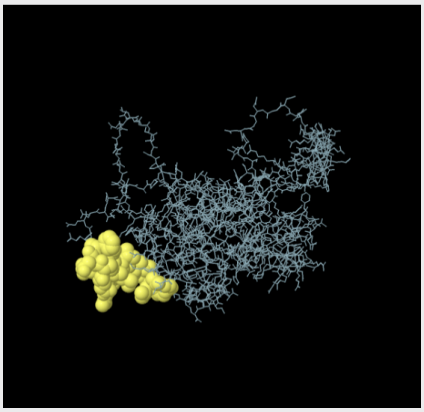

No.	Residues	Number of Residues	Score	3D Structure
9	A:S21, A:N23, A:A24, A:A26, A:K27, A:S28, A:F29, A:E30, A:R31, A:S32, A:L33, A:G34, A:H35 (SNAAKSFERSLGH)	13	0.648	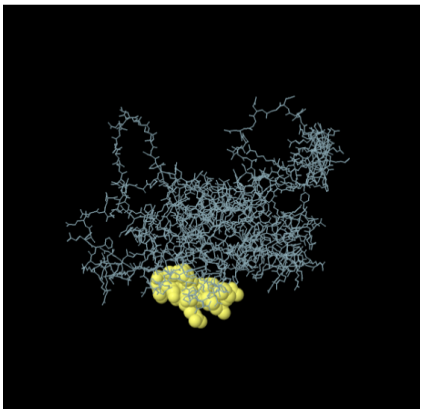
10	A:F148, A:L152, A:V153, A:D154, A:W155, A:E156, A:N157, A:K160, A:G161, A:S162, A:P163, A:E164, A:P165, A:D166, A:D167, A:R169, A:S170, A:Q173 (FLVDWENKGSPEPDDRSQ)	18	0.589	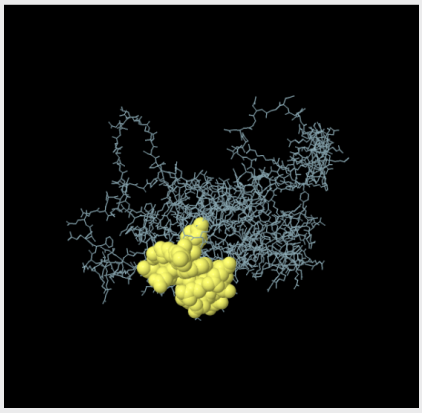
11	A:L140, A:D142, A:R143, A:C144, A:L145, A:Q146, A:Q147, A:R149, A:E150, A:Q151, A:E174, A:L176, A:A177, A:N178, A:Q179, A:S180, A:A183, A:D223, A:I225, A:P226, A:G227, A:C228, A:A229, A:A230, A:L231 (LDRCLQQREQELANQSADIPG-CAAL)	25	0.581	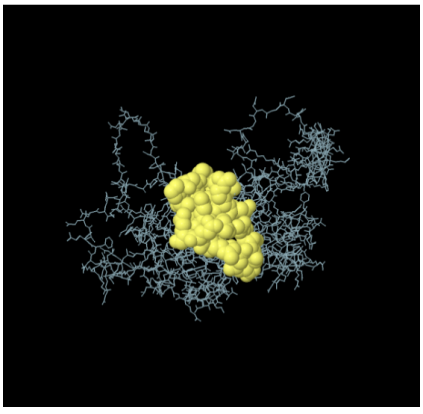
12	A:E259, A:G262, A:R263, A:A265, A:R266, A:E267, A:R281 (EGRARER)	7	0.559	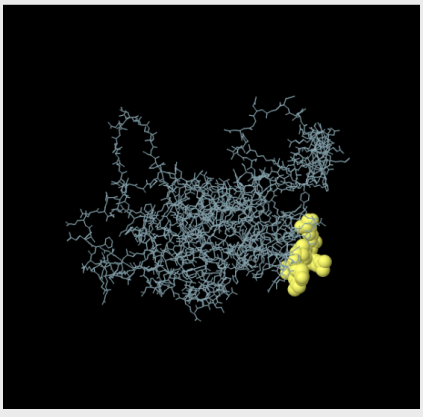

No.	Residues	Number of Residues	Score	3D Structure
13	A:E268, A:P269, A:S270, A:A272, A:G273, A:R274 (EPSAGR)	6	0.516	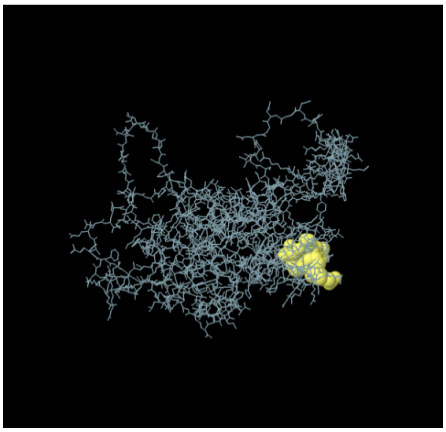
14	A:G284, A:L285, A:T286 (GLT)	3	0.505	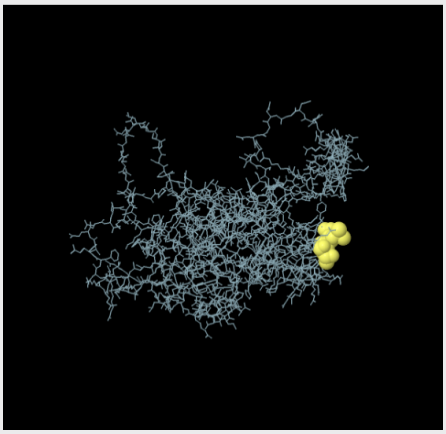

Table 5. IC_{50} values for ROP13 binding to MHC class I molecules obtained using the IEDB[a]

MHC I Allele[a]	Start-stop[c] ROP13	Peptide Sequence	Percentile Rank[d] ROP13
H2-D[b]	43-52	SSPLNSDVEL	0.165
H2-D[b]	6-15	SAPQELVDHL	0.4
H2-D[b]	18-27	CAALSLPAYI	0.44
H2-D[d]	57-66	RDPRRLSFPV	0.545
H2-D[d]	7-16	RPPGRKYEGS	1.4
H2-D[d]	5-14	LTPERQTFYQ	1.8
H2-K[b]	41-50	VVYANSLRLL	0.355
H2-K[b]	27-36	KSFERSLGHL	0.47
H2-K[b]	10-19	QTFYQPFVFV	2.2
H2-K[d]	27-34	AYIGLVSSDV	0.35
H2-K[d]	39-48	QSFGALHTTV	2.85
H2-K[d]	26-35	KYRRLRRQAA	3.35
H2-Kk	34-43	EEWEQRKASR	7.65
H2-Kk	21-30	TQAAMLLSMV	9.2

MHC I Allele[a]	Start-stop[c] ROP13	Peptide Sequence	Percentile Rank[d] ROP13
H2-Kk	28-37	SFERSLGHLD	10.8
H2-L[d]	33-42	HPFLSILVNM	0.74
H2-L[d]	14-23	RIPGCAALSL	2.6
H2-L[d]	2-11	VPLDSAPQEL	2.7

[a]The immune epitope database [49], [b]H2-Db, H2-Dd, H2-Kb, H2-Kd, H2-Kk, and H2-Ld alleles are mouse MHC class I molecules, [c]Ten amino acids were used for each analysis, [d]Low percentile rank = high binding affinity; high percentile rank = low binding affinity.

Note: IC_{50} values are presented as percentile rank.

Table 6. IC_{50} values for ROP13 binding to MHC class II molecules obtained using the IEDB[a]

MHC II Allele[b]	Start-stop ROP13[c]	Peptide Sequence	Percentile Rank ROP13[d]
H2-IA[b]	13-27	AVGAFAFTSPNAVAK	0.01
H2-IA[b]	15-29	GAFAFTSPNAVAKSF	0.01
H2-IA[b]	36-50	LDASSFLSSPLNSDV	1.96
H2-IA[d]	4-18	TELCIAALVAVGAFA	1.23
H2-IA[d]	6-20	LCIAALVAVGAFAFT	1.8
H2-IA[d]	30-44	LRRQAANVAAQVVYA	2.27
H2-IE[d]	20-34	KLLFLRKYRRLRRQA	0.05
H2-IE[d]	17-31	MYLKLLFLRKYRRLR	0.15
H2-IE[d]	24-38	LRKYRRLRRQAANVA	1.09

[a]The immune epitope database [50], bH2-IAb, H2-IAd, and H2-IEd alleles are mouse MHC class II molecules, [c]Fifteen amino acids were used for each analysis, [d]Low percentile rank = high binding affinity; high percentile rank = low binding affinity.
Note: IC_{50} values are presented as percentile rank.

Table 7. Predicted ROP13 epitopes using CTLpred[a]

Peptide Rank	Start Position[b]	Sequence	Score (ANN/SVM)[c]	Prediction
1	258	SEDFGRSAR	0.99/0.91	Epitope
2	223	DRIPGCAAL	0.43/1.28	Epitope
3	217	KLKHLLDRI	0.90/0.76	Epitope
4	133	SFPSQRRLL	0.97/0.65	Epitope
5	253	KVNRCSEDF	0.96/0.61	Epitope
6	374	LRKYRRLRR	0.67/0.85	Epitope
7	187	TVISFSIFV	0.51/1.00	Epitope
8	132	TSFPSQRRL	0.44/1.05	Epitope
9	277	AVVIRFMGL	0.04/1.44	Epitope
10	334	IREVLLRAL	0.24/1.23	Epitope

[a]CTLpred, [53], [b]Nine amino acids were used for each analysis, [c]The default ANN and SVM cut-off scores were set at 0.51 and 0.36, respectively.

The current investigation was performed to analyze and compare the different aspects of the ROP13 protein using bioinformatics techniques and online servers to design a suitable toxoplasmosis vaccine. The present research employed multiple bioinformatic tools to assess the diverse features of ROP13. It is indicated that peptides with a MW of <5–10 KDa are regarded as poorly immunogenic [67]. Herein, it has been found that the amino acid sequence of the ROP13 protein comprises 400 residues and an average MW of 44,714.15 D, suggesting a good antigenic nature.

Our analysis showed that the aliphatic index and GRAVY score of the ROP13 sequence were calculated as 84.40 and -0.311, respectively. A high aliphatic index shows that the target protein is stable over a broad spectrum of temperatures. The negative or low GRAVY score suggests that the peptide has better interaction with surrounding water molecules. It is widely recognized that ROPs contain an N-terminal signal sequence and a C-terminal hydrophobic sequence, which is believed to include a TM [69].

In this study, we observed that there was only one TMs in the *ROP13* gene sequence. Studies have indicated that PTM sites serve as a set of enzymatic functions capable of modulating the function, structure, and stability of proteins [71]. Accordingly, we identified acylation and phosphorylation sites on the ROP13 protein. Our findings revealed a total of 43 PTM sites (two acylation and 41 phosphorylation positions) within the sequence. These sites suggest the potential modulation of protein function, which could influence its activity.

It is well established that the secondary structure of proteins depends on the hydrogen bond pattern between amino hydrogen atoms and carboxyl oxygen atoms in a polypeptide chain, with alpha helices and beta sheets being the most common structures [72]. Proteins play a crucial role in the body due to their 3D shape. Understanding the correlation between protein structure and function is essential. Therefore, determining the tertiary structure of proteins is a key step in unraveling their functional properties [71]. Our investigation into the secondary structure of ROP13 revealed that it contains 40% alpha helix, 9.25% extended strand, and 50.75% random coil. The Ramachandran plot revealed that 91.8% of amino acid residues were located in the ideal regions, with 7.6% and 0.6% found in the allowed and disallowed regions of the plot, respectively.

Several studies have demonstrated that immunization against T. gondii infection is conferred through acquired immune responses, including humoral and cellular immunity, as well as regulatory cytokines [73-76]. Specific IgG antibodies, acting as anti-Toxoplasma antibodies, effectively control and limit parasite growth [74]. They interfere with parasite replication by limiting its adhesion to surface receptors on host cells and inhibiting the functions of parasite proteins [74, 75]. They also stimulate macrophage phagocytosis, which enhances the body's immune response against intracellular parasitic infections [75, 76]. Additionally, the secretion of interferon-γ (IFN-γ) by CD4+ and CD8+ T cells is a critical indicator of cellular response generation. This response is essential for preventing the reactivation of bradyzoites within host tissue cysts [75, 76]. In addition, epitope identification is helpful as it directly induces a robust immunity to properly control the parasite in vaccine design research [71]. In silico B-cell epitope mapping enables a better understanding of epitopes that are essential with regard to the interactions that happen between antibodies and pathogens.

The continuous B-cell epitope prediction results revealed that the ROP13 protein contains positive epitopes with acceptable indices, as determined using the Bcepred online server. Subsequently, we utilized this server to identify B-cell epitopes based on various physicochemical characteristics including accessibility, hydrophilicity, flexibility/ mobility, exposed surface, polarity, turns, or a combination of these properties [19].

The lower IC_{50} values indicate a higher affinity for MHC binding, suggesting an appropriate T-cell epitope. The analysis of IC_{50} values of peptides from the IEDB output indicates that the T-cell epitopes on ROP13 can strongly bind to MHC class I and class II molecules.

5. Conclusion

This research provides insights into the potential role of the ROP13 protein in combating *T. gondii* infection, supported by bioinformatics analyses. However, further experimental validation is needed to definitively assess its effectiveness. The goal of such studies is to fully comprehend the role of the ROP13 protein in preventing *T. gondii* infection, which requires conducting comprehensive experimental studies and gathering more information.

Acknowledgements

The authors sincerely thank the personnel from the Medical Microbiology Research Center, Qazvin University of Medical Sciences, Qazvin, Iran, and Jahrom University of Medical Sciences, Jahrom, Iran.

Compliance with ethical guidelines

This study was approved by the Research Ethics Committee of Qazvin University of Medical Sciences, Qazvin, Iran (Code: IR.QUMS.REC.1400.481).

Data availability

The datasets used and/or analyzed during the current study are available from the corresponding author upon reasonable request.

Funding

This research was supported by the Medical Microbiology Research Center, Qazvin University of Medical Sciences, Qazvin, Iran (R: 22247). The funder of the study had no role in the study design, data collection, data analysis, data interpretation, or writing of the report.

Authors' contributions

Study design: Milad Badri, Aida Vafae Eslahi, Masoud Foroutan and Leila Zaki; Data collection, data acquisition, and investigation: Milad Badri, Mohammad Ghaffari Cherati, Amir Karimipour-Saryazdi, Daniel Diaz, and Majid Pirestani; Writing the original draft: Milad Badri, Leila Zaki and Aida Vafae Eslahi; Review and editing: Milad Badri, Kareem Hatam-Nahavandi, and Aida Vafae Eslahi; Data analysis: Daniel Diaz, Milad Badri Aida Vafae Eslahi and Masoud Foroutan; Final approval: All authors.

Conflict of interest

The authors declared no conflict of interest.

References

[1] Rostami A, Riahi SM, Gamble HR, Fakhri Y, Nourollahpour Shiadeh M, Danesh M, et al. Global prevalence of latent toxoplasmosis in pregnant women: A systematic review and meta-analysis. Clin Microbiol Infect. 2020; 26(6):673-83. [DOI:10.1016/j.cmi.2020.01.008] [PMID]

[2] Abbasali Z, Pirestani M, Dalimi A, Badri M, Fasihi-Ramandi M. Anti-parasitic activity of a chimeric peptide Cecropin A (2-8)-Melittin (6-9)(CM11) against tachyzoites of Toxoplasma gondii and the BALB/c mouse model of acute toxoplasmosis. Mol Biochem Parasitol. 2023; 255:111578. [DOI:10.1016/j.molbiopara.2023.111578] [PMID]

[3] Rojas-Barón L, Tana-Hernandez L, Nguele Ampama MH, Sanchéz R, Gärtner U, Wagenlehner FME,et al. Adverse impact of acute Toxoplasma gondii infection on human spermatozoa. FEBS J. 2025; 292(17):4720-36. [PMID]

[4] Sanchez SG, Besteiro S. The pathogenicity and virulence of Toxoplasma gondii. Virulence. 2021; 12(1):3095-114. [DOI:10.1080/21505594.2021.2012346] [PMID]

[5] Haghbin M, Maani S, Bagherzadeh MA, Bazmjoo A, Shakeri H, Taghipour A, et al. Latent Toxoplasmosis among Breast Cancer Patients in Jahrom, South of Iran. Int J Breast Cancer. 2023; 2023:4792260. [DOI:10.1155/2023/4792260] [PMID]

[6] Dubey JP. The history of Toxoplasma gondii the first 100 years. J Eukaryot Microbiol. 2008; 55(6):467-75. [DOI:10.1111/j.1550-7408.2008.00345.x] [PMID]

[7] Wang ZD, Liu HH, Ma ZX, Ma HY, Li ZY, Yang ZB, et al. Toxoplasma gondii infection in immunocompromised patients: A systematic review and meta-analysis. Front Microbiol. 2017; 8:389. [DOI:10.3389/fmicb.2017.00389] [PMID]

[8] Mose JM, Kagira JM, Kamau DM, Maina NW, Ngotho M, Karanja SM, et al. A review on the present advances on studies of toxoplasmosis in eastern Africa. Biomed Res Int. 2020; 2020:7135268. [DOI:10.1155/2020/7135268] [PMID]

[9] Dupont CD, Christian DA, Hunter CA. Immune response and immunopathology during toxoplasmosis. Semin Immunopathol. 2012; 34(6):793-813. [DOI:10.1007/s00281-012-0339-3] [PMID]

[10] Abdoli A, Olfatifar M, Eslahi AV, Moghadamizad Z, Samimi R, Habibi MA, et al. A systematic review and meta-analysis of protozoan parasite infections among patients with mental health disorders: An overlooked phenomenon. Gut Pathog. 2024;16(1):7. [DOI:10.1186/s13099-024-00602-2] [PMID]

[11] Gharavi MJ, Jalali S, Khademvatan S, Heydari S. Detection of IgM and IgG anti-Toxoplasma antibodies in renal transplant recipients using ELFA, ELISA and ISAGA methods: Comparison of pre-and post-transplantation status. Ann Trop Med Parasitol. 2011; 105(5):367-71. [DOI:10.1179/136485911Y.0000000022] [PMID]

[12] Weiss LM, Dubey JP. Toxoplasmosis: A history of clinical observations. Int J Parasitol. 2009; 39(8):895-901. [DOI:10.1016/j.ijpara.2009.02.004] [PMID]

[13] Tenter AM. Toxoplasma gondii in animals used for human consumption. Mem Inst Oswaldo Cruz. 2009; 104(2):364-9. [DOI:10.1590/S0074-02762009000200033] [PMID]

[14] Hajj RE, Tawk L, Itani S, Hamie M, Ezzeddine J, El Sabban M, et al. Toxoplasmosis: Current and emerging parasite druggable targets. Microorganisms. 2021; 9(12):2531. [DOI:10.3390/microorganisms9122531] [PMID]

[15] Antczak M, Dzitko K, Dugoska H. Human toxoplasmosis Searching for novel chemotherapeutics. Biomed Pharmacother. 2016; 82:677-84. [DOI:10.1016/j.biopha.2016.05.041] [PMID]

[16] Pagheh AS, Sarvi S, Sharif M, Rezaei F, Ahmadpour E, Dodangeh S, et al. Toxoplasma gondii surface antigen 1 (SAG1) as a potential candidate to develop vaccine against toxoplasmosis: A systematic review. Comp Immunol Microbiol Infect Dis. 2020; 69:101414. [DOI:10.1016/j.cimid.2020.101414] [PMID]

[17] Zhang NZ, Chen J, Wang M, Petersen E, Zhu XQ. Vaccines against Toxoplasma gondii: New developments and perspectives. Expert Rev Vaccines. 2013; 12(11):1287-99. [DOI:10.1586/14760584.2013.844652] [PMID]

[18] Rezaei F, Sarvi S, Sharif M, Hejazi SH, Pagheh AS, Aghayan SA, et al. A systematic review of Toxoplasma gondii antigens to find the best vaccine candidates for immunization. Microb Pathog. 2019; 126:172-84. [DOI:10.1016/j.micpath.2018.11.003] [PMID]

[19] Kazi A, Chuah C, Majeed ABA, Leow CH, Lim BH, Leow CY. Current progress of immunoinformatics approach harnessed for cellular-and antibody-dependent vaccine design. Pathog Glob Health. 2018; 112(3):123-31. [DOI:10.1080/20477724.2018.1446773] [PMID]

[20] Dlugonska H. Toxoplasma rhoptries: Unique secretory organelles and source of promising vaccine proteins for immunoprevention of toxoplasmosis. J Biomed Biotechnol. 2008; 2008:632424. [DOI:10.1155/2008/632424] [PMID]

[21] Pagheh AS, Daryani A, Alizadeh P, Hassannia H, Rodrigues Oliveira SM, Kazemi T, et al. Protective effect of a DNA vaccine cocktail encoding ROP13 and GRA14 with Alum nano-adjuvant against Toxoplasma gondii infection in mice. Int J Biochem Cell Biol. 2021; 132:105920. [DOI:10.1016/j.biocel.2021.105920] [PMID]

[22] Turetzky JM, Chu DK, Hajagos BE, Bradley PJ. Processing and secretion of ROP13: A unique Toxoplasma effector protein. Int J Parasitol. 2010; 40(9):1037-44. [DOI:10.1016/j.ijpara.2010.02.014] [PMID]

[23] Wang PY, Yuan ZG, Petersen E, Li J, Zhang XX, Li XZ, et al. Protective efficacy of a Toxoplasma gondii rhoptry protein 13 plasmid DNA vaccine in mice. Clin Vaccine Immunol. 2012; 19(12):1916-20. [DOI:10.1128/CVI.00397-12] [PMID]

[24] Kang HJ, Lee SH, Kim MJ, Chu KB, Lee DH, Chopra M, et al. Influenza virus-like particles presenting both Toxoplasma gondii ROP4 and ROP13 Enhance Protection against T. gondii infection. Pharmaceutics. 2019; 11(7):342. [DOI:10.3390/pharmaceutics11070342] [PMID]

[25] Zhou J, Wang L, Zhou A, Lu G, Li Q, Wang Z, et al. Bioinformatics analysis and expression of a novel protein ROP48 in Toxoplasma gondii. Acta Parasitol. 2016; 61(2):319-28. [DOI:10.1515/ap-2016-0042] [PMID]

[26] Romano P, Giugno R, Pulvirenti A. Tools and collaborative environments for bioinformatics research. Brief Bioinform. 2011; 12(6):549-61. [DOI:10.1093/bib/bbr055] [PMID]

[27] National Center for Biotechnology Information (NCBI). amino acid sequence of ROP13. National Center for Biotechnology Information; 2025. [Link]

[28] Expasy. The Expasy ProtParam tool. Vaud: SIB Swiss Institute of Bioinformatics; 2025. [Link]

[29] Gasteiger E, Hoogland C, Gattiker A, Duvaud S, Wilkins MR, Appel RD, et al. Protein identification and analysis tools on the ExPASy server. In: Walker JM, editor. The Proteomics Protocols Handbook. Springer Protocols Handbooks. New Jersey: Humana Press. [DOI:10.1385/1-59259-890-0:571]

[30] No Auther. The online tools NetPhos 3.1 [Internet]. 2025 [Updated 26 November 2025]. Available from: [Link]

[31] No Auther. CSS-Palm. [Internet]. 2025 [Updated 26 November 2025]. Available from: [Link]

[32] DTU. TMHMM-2.0. Kongens Lyngby: Technical University of Denmark; 2025. [Link]

[33] PSORT. PSORT II Prediction [Internet]. 1999 [Updated 24 November 1999]. Available from: [Link]

[34] NPSA. The secondary structure of ROP13 was predicted using the Garnier-Osguthorpe-Robson (GOR) method through the online server. 2025.

[35] Garnier J, Gibrat JF, Robson B. GOR method for predicting protein secondary structure from amino acid sequence. Methods Enzymol. 1996; 266:540-53. [DOI:10.1016/S0076-6879(96)66034-0] [PMID]

[36] SWISS-MODEL. SWISSMODEL program [Internet]. 2025 [Updated 26 November 2025]. Available from: [Link]

[37] Guex N, Peitsch MC, Schwede T. Automated comparative protein structure modeling with SWISS-MODEL and Swiss-PdbViewer: A historical perspective. Electrophoresis. 2009; 30(S1):S162--73. [DOI:10.1002/elps.200900140] [PMID]

[38] UCLA-DOE LAB — SAVES v6.1. PROCHECK tool [Internet]. 2025 [Updated 26 November 2025]. Available from: [Link]

[39] Foroutan M, Karimipour-Saryazdi A, Ghaffari AD, Majidiani H, Arzani Birgani A, Karimzadeh-Soureshjani E, et al. In Silico Analysis and Characterization of the Immunogenicity of Toxoplasma gondii Rhoptry Protein 18. Bioinform Biol Insights. 2025; 19:11779322251315924. [DOI:10.1177/11779322251315924] [PMID]

[40] Laskowski RA, Rullmannn JA, MacArthur MW, Kaptein R, Thornton JM. AQUA and PROCHECK-NMR: Programs for checking the quality of protein structures solved by NMR. J Biomol NMR. 1996; 8(4):477-86. [DOI:10.1007/BF00228148] [PMID]

[41] Computational Resources for Drug Discovery. ABCpred server. [Internet]. 2025 [Updated 26 November 2025]. Available from: [Link]

[42] Saha S, Raghava GP. Prediction of continuous B-cell epitopes in an antigen using recurrent neural network. Proteins. 2006; 65(1):40-8. [DOI:10.1002/prot.21078] [PMID]

[43] Computational Resources for Drug Discovery. Bcepred tool. 2025.

[44] Saha S, Raghava GPS. BcePred: prediction of continuous B-cell epitopes in antigenic sequences using physico-chemical properties. Paper presented at: International Conference on Artificial Immune Systems. September 13-16, 2004; Catania, Sicily, Italy. [Link]

[45] IEDB Analysis Resource. IEDB tool [Internet]. 2025 [Updated 26 November 2025]. Available from: [Link]

[46] IEDB Analysis Resource. ElliPro [Internet]. 2025 [Updated 26 November 2025]. Available from: [Link]

[47] Ponomarenko J, Bui HH, Li W, Fusseder N, Bourne PE, Sette A, et al. ElliPro: A new structure-based tool for the prediction of antibody epitopes. BMC Bioinformatics. 2008; 9:514. [PMID]

[48] The Immune Epitope Database (IEDB). Assess the half maximal inhibitory concentration (IC50) of peptides derived from ROP13 that exhibit af finity to both major histocompatibility complex (MHC) class I and class II molecules [Internet]. 2025 [Updated 26 November 2025]. Available from: [Link]

[49] IEDB Analysis Resource. MHC-I Binding Predictions [Internet]. 2025 [Updated 26 November 2025]. Available from: [Link]

[50] IEDB Analysis Resource. MHC class II [Internet]. 2025 [Updated 26 November 2025]. Available from: [Link]

[51] Wang P, Sidney J, Dow C, Mothé B, Sette A, Peters B. A systematic assessment of MHC class II peptide binding predictions and evaluation of a consensus approach. PLoS Comput Biol. 2008; 4(4):e1000048. [DOI:10.1371/journal.pcbi.1000048] [PMID]

[52] Wang P, Sidney J, Kim Y, Sette A, Lund O, Nielsen M, et al. Peptide binding predictions for HLA DR, DP and DQ molecules. BMC Bioinformatics. 2010; 11:568. [PMID]

[53] Bio.tools. CTLpred tool. [Internet]. 2025 [Updated 26 November 2025]. Available from: [Link]

[54] Bhasin M, Raghava GP. Prediction of CTL epitopes using QM, SVM and ANN techniques. Vaccine. 2004; 22(23-24):3195-204. [DOI:10.1016/j.vaccine.2004.02.005] [PMID]

[55] Scratch Protein Predictor. ANTI¬GENpro [Internet]. 2025 [Updated 26 November 2025]. Available from: [Link]

[56] Magnan CN, Zeller M, Kayala MA, Vigil A, Randall A, Felgner PL, et al. High-throughput prediction of protein antigenicity using protein microarray data. Bioinformatics. 2010; 26(23):2936-43. [DOI:10.1093/bioinformatics/btq551] [PMID]

[57] The Edward Jenner Institute for Vaccine Research. VaxiJen v. 2.0. [Internet]. 2025 [Updated 26 November 2025]. Available from: [Link]

[58] Doytchinova IA, Flower DR. VaxiJen: A server for prediction of protective antigens, tumour antigens and subunit vaccines. BMC Bioinformatics. 2007; 8:4. [PMID]

[59] AlgPred. Allergenic profile of ROP13 was predicted using the AlgPred [Internet]. 2025 [Updated 26 November 2025].

[60] Saha S, Raghava GP. AlgPred: Prediction of allergenic proteins and mapping of IgE epitopes. Nucleic Acids Res. 2006; 34(Web Server issue):W202-9. [PMID]

[61] Magnan CN, Randall A, Baldi P. SOLpro: Accurate sequence-based prediction of protein solubility. Bioinformatics. 2009; 25(17):2200-7. [DOI:10.1093/bioinformatics/btp386] [PMID]

[62] C-IMMSIM. C-ImmSim was employed to simulate the virtual immunological response triggered by TgROP13 [Internet]. 2025 [Updated 26 November 2025]. Available from: [Link]

[63] Kur J, Holec-Gasior L, Hiszczyńska-Sawicka E. Current status of toxoplasmosis vaccine development. Expert Rev Vaccines. 2009; 8(6):791-808. [DOI:10.1586/erv.09.27] [PMID]

[64] Dodangeh S, Fasihi-Ramandi M, Daryani A, Valadan R, Sarvi S. In silico analysis and expression of a novel chimeric antigen as a vaccine candidate against Toxoplasma gondii. Microb Pathog. 2019; 132:275-81. [DOI:10.1016/j.micpath.2019.05.013] [PMID]

[65] Berzofsky JA. Immunogenicity and antigen structure. Fundam Immunol. 1993; 235–82. [Link]

[66] El Hajj H, Demey E, Poncet J, Lebrun M, Wu B, Galéotti N, et al. The ROP2 family of Toxoplasma gondii rhoptry proteins: proteomic and genomic characterization and molecular modeling. Proteomics. 2006; 6(21):5773-84. [DOI:10.1002/pmic.200600187]

[67] Walsh C. Posttranslational modification of proteins: Expanding nature's inventory. York City: W. H. Freeman and Company; 2006. [Link]

[68] DTU Health Tech. Number of predicted TMHs. DTU Health Tech; 2025. [Link]

[69] Yada RY, Jackman RL, Nakai S. Secondary structure prediction and determination of proteins: A review. Int J Pept Protein Res. 1988; 31(1):98–108. [DOI:10.1111/j.1399-3011.1988.tb00011.x]

[70] NPSA. Predicted secondary structure by the GOR IV online service. [Internet]. 2025 [Updated 26 November 2025]. Available from: [Link]

[71] Wang Y, Wang G, Cai J, Yin H. Review on the identification and role of Toxoplasma gondii antigenic epitopes. Parasitol Res. 2016; 115(2):459-68. [DOI:10.1007/s00436-015-4824-1] [PMID]

[72] Zaki L, Ghaffarifar F, Sharifi Z, Horton J, Sadraei J. Effect of Imiquimod on Tachyzoites of Toxoplasma gondii and Infected Macrophages in vitro and in BALB/c Mice. Front Cell Infect Microbiol. 2020; 10:387. [DOI:10.3389/fcimb.2020.00387] [PMID]

[73] Zaki L, Ghaffarifar F, Sharifi Z, Horton J, Sadraei J. Toxoplasma gondii: Preventive and therapeutic effects of morphine and evaluation of treatment parameters of tachyzoites and infected macrophages in vitro and in a murine model. EXCLI J. 2020; 19:514-27. [PMID]

[74] Sayles PC, Gibson GW, Johnson LL. B cells are essential for vaccination-induced resistance to virulent Toxoplasma gondii. Infect Immun. 2000; 68(3):1026-33. [DOI:10.1128/IAI.68.3.1026-1033.2000] [PMID]

[75] El-Kady IM. T-cell immunity in human chronic toxoplasmosis. J Egypt Soc Parasitol. 2011; 41(1):17-28. [PMID]

[76] Suzuki Y, Orellana MA, Schreiber RD, Remington JS. In- terferon-gamma: The major mediator of resistance against Toxoplasma gondii. Science. 1988; 240(4851):516-8. [DOI:10.1126/science.3128869] [PMID]